Data-driven Dynamic Programming: a Peak Shaving Application

Francisca Mestre

Master of Science Thesis

TU Delft Delft University of Technology

Delft Center for Systems and Control

Data-driven Dynamic Programming: a Peak Shaving Application

Master of Science Thesis

For the degree of Master of Science in Systems and Control at Delft University of Technology

Francisca Mestre

November 10, 2020

Faculty of Mechanical, Maritime and Materials Engineering (3mE) · Delft University of Technology

Abstract

The rising number of electricity consumers poses a challenge to power generators and grid operators in maintaining a balanced grid. Peak shaving is a technique that consists of shifting electricity consumption from hours of high demand to times of low demand, and has been gaining popularity in recent years. It allows to reduce peak loads which must be met at all times, which in turn reduces the need to resort to less efficient and more expensive power plants to see that all peaks are met. This paper proposes two methods to operate a battery energy storage system (BESS) for peak shaving of daily load profiles, based on the dynamic programming (DP) algorithm. The first approach treats historical profiles as deterministic paths and solves the DP algorithm for each profile. Then, an operating plan is obtained in real-time by combining the policies calculated for each path. The second approach treats data as stochastic paths, from which it derives a probabilistic model for the target path. Given this model, the DP algorithm obtains an operating plan for the entire day ahead. We also propose three modifications that can be applied to the two methods which aim at the improving the reliability of the methods. The performance of the proposed methods is examined through numerical experiments on both artificial and real data.

Keywords: Dynamic programming, peak shaving, battery energy storage system (BESS).

Table of Contents

List of Figures

List of Tables

Acknowledgements

This thesis would not have been possible without the support of my supervisors. Peyman Mohajerin Esfahani, thank you for all your guidance and advice throughout this time. Amin Kolarijani, thank you for reading this thesis several times, for all your amazing suggestions and for pushing me to do better.

To my friends, for all the laughs we had together during the past years, but also for having my back on the not-so-good times. To Ana Pereira, for being the best group assignment partner anyone could ask for. To Carolina Barata for always taking my calls when I need to talk. To my incredible housemates, who took me in when I first moved to a different country.

To my family, for all their support and patience. Mom, Dad and Ana, for being there for whatever I need and for distracting me. To my grandparents, for all their endless love. Avó, I wish you could be here to see this. To our pets, who can offer so much support without a single word.

And to Zé, who is never not there. For understanding when I'm upset and for being able to turn my mood around, even when I do not really want it. For listening to me when I need to think out loud. For all the movie nights, which are the best.

Delft, University of Technology — Francisca Mestre
November 10, 2020

Chapter 1

Introduction

The power grid is a network for distributing electricity from producers to consumers. In a simplistic manner, electricity is produced in generating stations (e.g. power plants, solar plants) and fed into the grid. Consumers buy electricity from the grid to meet their power demand. Maintaining a balance between electricity generation (supply) and load (demand) is crucial for a stable and cost-effective energy system [1, 2, 3, 4]. The increasing number of end-consumers [5] of electricity increases the risk of a power failure which occurs if the grid cannot meet the demand [6], particularly in times of peak demand. In order to avoid power failures, utility companies resort to peaking generators to meet peak demand, which implies increased maintenance and operation costs [7, 8], and grid operators are forced to purchase electricity from more expensive sources [6]. The peaking generators are often less efficient and emit more greenhouse gas (GHG) into the atmosphere [9]. Furthermore, the extra costs result in an increased cost of supply which is covered by the consumers in the form of time-varying energy consumption fees and peak fees. The electricity bill of the consumer over a period T is calculated by [10]

$$\sum_{t=0}^{T} E\left(t\right) E_{fee}\left(t\right) + p_T p_{fee} \tag{1-1}$$

where $E(t)$ is the energy consumption at each time step $t \in \{0, 1, \ldots, T\}$, E_{fee} is the energy fee at time t, p_T is the peak load observed over T time steps and p_{fee} is the fee associated to the peak load.

Demand side management (DSM) [3, 11] provides a collection of measures, taken on the demand side of the energy system, that aim at improving the energy efficiency of buildings and devices. These measures can be as simple as replacing lightbulbs with more efficient ones up to reshaping the load profiles with sophisticated control techniques.

Peak shaving, which is the process of shifting electricity consumption from hours of high demand to times of low demand, is one DSM measure that has been gaining popularity in recent years, particularly when implemented via a battery energy storage system (BESS) [12, 2]. It can, potentially, provide a number of advantages for the grid operator, the end-user and in regard to GHG emissions [13, 14]. Battery storage may help to maintain a balanced grid

[15]. Furthermore, if peak loads decrease, the need to resort to inefficient peaking generators is also decreased, improving power quality and cutting GHG emissions. The end-user's bill, in turn, is reduced not only because its peak load is now lower, but also because it is not being charged the extra costs of using peaking generators, which assume the form of $E_{fee}(t)$ in Eq. (1-1).

The concept of shaving the peaks of a consumer's electricity patterns with a BESS is presented in Figure 1-1 and Figure 1-1b. Figure 1-1a shows how the BESS is integrated between the grid and the end-user. Without an intermediate actor, the load that the consumer imposes on the grid is equal to the consumer demand at each time step. This means that, throughout a period of time T, the maximum power demand observed by the consumer will coincide with the maximum load imposed on the grid. However, once the BESS is operating between grid and consumer, load and demand become different quantities. From this point onward, there is an important distinction to make between the terms "load" and "demand". We will refer to the power required by an electricity user at any instant by "demand" and to the power that that user imposes on the grid as "load". This distinction is made clear in Figure 1-1b. When the battery is charging, the grid supplies power to the consumer and to the battery, so load is greater than demand. When the battery is discharging, part of the consumer demand is met by the battery, therefore the load seen by the grid is lower than the demand.

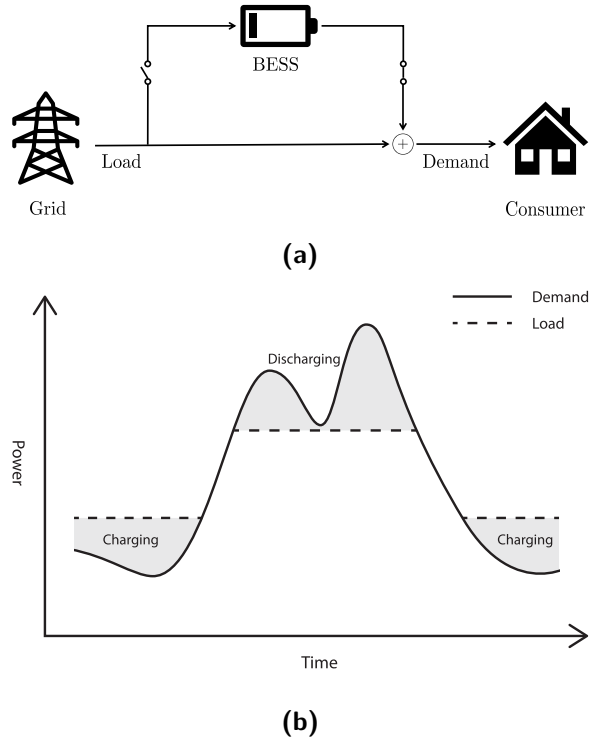

Figure 1-1: Peak shaving with BESS. (a) The BESS is an actor between the grid and the consumer. (b) The full line is the demand profile, and the dashed line is the load profile seen by the grid.

Several studies have been conducted which focus on using BESS for peak shaving. In general, they can be split in two main groups [13]: optimal sizing of the battery [12, 16, 17] and

optimal operation. This work will focus on the latter. In [18], upper demand limits (DL) were established and the battery was given discharge commands when demand was above the DL. In [19] and [20], DL were also established, as well as upper and lower limits on the state of charge (SoC) of the battery to extend its lifetime. In [21], an algorithm for calculating the optimal DL from historical data is proposed. In [16], the authors propose an optimal operation schedule for the BESS which is obtained from a dynamic program. The dynamic program requires a DL as input and operates the BESS such that the DL is not exceeded. From simulation the authors conclude that this method is ineffective for long peaks. In [22], a real-time control strategy to shave the peak and smooth the load curve is proposed. This control strategy relies on forecasts of the load curve.

Contributions This work focuses mainly on the consumer's side, and it proposes two methods to shave the peak load of electricity customers' daily load profiles. One of the main difficulties of peak shaving is that the demand curve, hence, the peaks, are not known in advance [10]. Both methods are built on the dynamic programming (DP) algorithm, due to its ability to deal with the unpredictable nature of the demand profiles as well as constraints on the controls [16], which will prove to be useful to this application. The two methods require that historical demand profiles are available and return a charge-discharge control policy. The first method treats historical data as deterministic paths and the battery's operating policy is obtained in real-time. The second method treats historical data as stochastic paths and the battery's operating policy is obtained prior to the beginning of the target day. This policy defines the strategy for the entire day ahead. Furthermore, this work also introduces three alterations that can be included in both methods to prevent peak increases that might occur, for instance, due to the stochastic behaviour of electricity consumption.

Organization of the thesis The remaining of this thesis is outlined as follows. In Chapter 2, the equations that describe the system composed of the grid, the consumer and the BESS are introduced and the control problem is modelled as a DP. In Chapter 3, the two methods are introduced, as well as the proposed alterations to prevent peak increases. In Chapter 4, we introduce the data set used in the simulations and show the results obtained with the two methods, without and with the proposed alterations. Moreover, the two methods are tested on artificially generated demand trajectories. In Chapter 5, two limiting factors of the peak shaving performance of both proposed methods are analysed. We also discuss the numerical aspects of both methods. Furthermore, the conclusions of this thesis are presented and future works are suggested to further develop and improve the proposed methods.

Chapter 2

Model and peak shaving problem

Dynamic programming (see [23, 24, 25]) plays an important role in both proposed methods. The DP algorithm requires that a model of the system to be controlled is available. In this chapter, the model of the system is presented and the peak shaving problem is formulated as an optimal control problem via DP.

2-1 Model of the system

As shown in Figure 1-1a, the system is composed of the electrical grid, the consumer and the BESS. In particular, Figure 1-1b shows the typical effect that peak shaving with a BESS has on the load curve imposed on the grid by the consumer.

The states of the system, i.e., the variables that describe the system at any point in time are:

- the state-of-charge (SoC) which is the ratio of the remaining energy in the battery at time t to its fully charged capacity, and it is represented by the variable c_t;
- the current consumer demand, represented by d_t;
- peak load seen by the grid so far, represented by p_t.

The SoC can take any real value between 0, when the battery is fully discharged, and 1, when it is fully charged. The demand and peak can take any real non-negative value. Thus, the state variable x_t and the state space $\mathbb{X}$ can be mathematically described as

$$x_t = (c_t, p_t, d_t) \in \mathbb{X} = [0, 1] \times \mathbb{R}_{\geq 0} \times \mathbb{R}_{\geq 0}. \tag{2-1}$$

The SoC dynamics are defined as

$$c_{t+1} = c_t + \max(u_t, 0) \cdot \overline{\alpha} + \min(u_t, 0) \cdot \underline{\alpha} \tag{2-2}$$

where $\overline{\alpha}$ and $\underline{\alpha}$ are charging and discharging coefficients, respectively, and u_t is the input given to the system. The battery receives charging commands if $u_t > 0$ and discharging commands if $u_t < 0$. Furthermore, the commands that the battery accepts at any given time are constrained by physical limits of the battery, $u^{\min}$ and $u^{\max}$, but also by its SoC —if the battery is fully charged it does not accept a charging command, and if it is fully discharged it does not accept a discharging command. Therefore, we have state-dependent constraints on the input variable. At the current time t with state $x_t = (c_t, p_t, d_t)$, the input constraints are described by

$$u_t \in \mathbb{U}(x_t) = \left[\max\left(u^{\min}, \frac{-c_t}{\underline{\alpha}}\right),\ \min\left(u^{\max}, \frac{1-c_t}{\overline{\alpha}}\right)\right]. \tag{2-3}$$

We write the dynamics of the power demand as

$$d_{t+1} = d_t + z_{t+1} \tag{2-4}$$

where d_t is the observed power demand at the current time step, and z_{t+1} is the exogenous information that represents the change in demand from the current time t to the next, and whose exact value is only revealed at the next time step. The exogenous information could also be taken to be the demand at the next time step itself, however, this notation will prove to be helpful in future sections. The exogenous information z_{t+1} is taken to be time-dependent. Indeed, the demand is more likely to rise rather than fall at certain times of the day while, at other times, it is more likely to fall. For instance, in an office building during the early hours of the morning the electricity consumption is more likely to increase as people arrive, rather than decrease. The distribution of the exogenous variable over a time period of T time steps is represented by

$$\Phi = \{\varphi_t\}_{t=0}^{T-1} \tag{2-5}$$

where $\varphi_t : \mathbb{R} \to \mathbb{R}_{\geq 0}$ is the probability density function of the exogenous information at time t.

The load seen by the grid at a certain time step, which is represented by the variable ℓ_t, differs from the actual demand by the same amount that is given as input to the battery, i.e.,

$$\ell_{t+1} = d_{t+1} + u_t = d_t + z_{t+1} + u_t. \tag{2-6}$$

Hence, the peak variable is updated if the load is larger than the peak seen so far by the grid:

$$p_{t+1} = \max(p_t, \ell_{t+1}) = \max(p_t, d_t + z_{t+1} + u_t). \tag{2-7}$$

The state update function f is then obtained by combining Eq. (2-2), Eq. (2-7) and Eq. (2-4):

$$f(x_t, u_t, z_{t+1}) = \begin{cases} c_{t+1} = c_t + \max(u_t, 0) \cdot \overline{\alpha} + \min(u_t, 0) \cdot \underline{\alpha} \\ p_{t+1} = \max(p_t, d_t + z_{t+1} + u_t) \\ d_{t+1} = d_t + z_{t+1} \end{cases}. \tag{2-8}$$

2-2 Peak shaving as a dynamic program

The peak shaving problem is formulated as an optimal control problem over a finite horizon via the DP algorithm. The aim of the DP algorithm is to minimize the total expected cost

$$\min_{u_0,\ldots,u_{T-1}} \mathop{\mathbb{E}}_{z_{t+1}} \left\{ G_T\left(x_T\right) + \sum_{t=0}^{T-1} g\left(x_t, u_t, z_{t+1}\right) \right\} \tag{2-9}$$

where $g\left(x_t, u_t\right)$ is the stage cost function and determines how each state transition is penalized, and $G_T\left(x_T\right)$ is the terminal cost function and determines how the final state is penalized.

In this work, the goal is to minimize the peak load that the consumer imposes on the grid over a finite period of time. Therefore, the stage cost function $g(x_t, u_t)$ is

$$g(x_t, u_t) = 0 \tag{2-10}$$

and terminal cost function $G_T(x_T)$ is

$$G_T(x_T) = p_T. \tag{2-11}$$

The stage cost function is zero because, in this work, we focus mainly on minimizing the peak. Nevertheless, it may be used to include time-of-use tariffs, or to minimize battery wear and stress.

Solving the problem in Eq. (2-9) is a complex and sometimes even intractable task [24]. The principle of optimality [26] allows for it to be split into T sub-problems:

1. $J_T^* = G_T\left(x_T\right), \ \ \forall x_T \in \mathbb{X}$

2. for $t = T-1, \ldots, 0, \ \ \forall x_t \in \mathbb{X}$:

$$J_t^*\left(x_t\right) = \min_{u_t \in \mathbb{U}_t(x_t)} \left(g_t(x_t, u_t) + \mathop{\mathbb{E}}_{z_{t+1}} \left\{ J_{t+1}^*\left(f\left(x_t, u_t, z_{t+1}\right)\right) \right\} \right) \tag{2-12}$$

$$\mu_t^*\left(x_t\right) \in \operatorname*{argmin}_{u_t \in \mathbb{U}_t(x_t)} \left(g_t(x_t, u_t) + \mathop{\mathbb{E}}_{z_{t+1}} \left\{ J_{t+1}^*\left(f\left(x_t, u_t, z_{t+1}\right)\right) \right\} \right).$$

These sub-problems are solved in a recursive manner: we start by calculating the value function J_T^* for the possible terminal states. Then, we solve the tail sub-problem for $T-1$ and obtain the value function J_{T-1}^* and the policy μ_{T-1}^*. Then, the sub-problem for $T-2$ and so on until $t = 0$. At this point a full value function $\{J_t^*\}_{t=0}^{T}$ and optimal policy $\{\mu_t^*\}_{t=0}^{T-1}$ are available.

2-2-1 Approximation via discretization

The states, decisions and exogenous information involved in the model are all continuous variables. There are several available methods to approximately solve a dynamic program

with continuous states, decision and random variables, such as in [24]. This work follows a common approach to deal with continuous variables in dynamic programming [27], [28]. It consists of quantizing the continuous variables into discrete subsets of the original spaces. Furthermore, it allows us to obtain the DP solution in the form of a look-up table that can be quickly queried at any time step. The continuous variables are quantized as follows:

- the SoC is quantized into a discrete subset $\mathbb{C}_s$ of N_c equidistant samples between 0 and 1:
$$\mathbb{C}_s = \left\{ \frac{j}{N_c - 1}, \;\; j = 0, \ldots, N_c - 1 \right\}; \tag{2-13}$$
- the demand is quantized into a discrete subset $\mathbb{D}_s$ of N_d equidistant samples between 0 and $d^{\max}$:
$$\mathbb{D}_s = \left\{ \frac{j \cdot d^{\max}}{N_d - 1}, \;\; j = 0, \ldots, N_d - 1 \right\}; \tag{2-14}$$
- the peak is quantized into a discrete subset $\mathbb{P}_s$ of N_p equidistant samples between 0 and $p^{\max}$:
$$\mathbb{P}_s = \left\{ \frac{j \cdot p^{\max}}{N_p - 1}, \;\; j = 0, \ldots, N_p - 1 \right\}; \tag{2-15}$$
- the decision is quantized into a discrete subset $\mathbb{U}_s$ of N_u equidistant samples between $u^{\min}$ and $u^{\max}$:
$$\mathbb{U}_s = \left\{ u^{\min} + \frac{j \cdot (u^{\max} - u^{\min})}{N_u - 1}, \;\; j = 0, \ldots, N_u - 1 \right\}. \tag{2-16}$$

We take $d^{\max} = p^{\max}$ to be the maximum demand value observed from data.

The discrete state subset is given by

$$\mathbb{X}_s = \mathbb{C}_s \times \mathbb{P}_s \times \mathbb{D}_s \tag{2-17}$$

and the state-dependent discrete input subset is given by

$$\mathbb{U}_s (x_t) = \mathbb{U}_s \cap \mathbb{U} (x_t). \tag{2-18}$$

Given that $g_t (x_t, u_t) = 0$, the DP recursion Eq. (2-12) can be rewritten as

1. $J_T = G_T (x_T), \;\; \forall x_T \in \mathbb{X}_s$

2. for $t = T - 1, \ldots, 0, \;\; \forall x_t \in \mathbb{X}_s$:

$$J_t (x_t) = \min_{u_t \in \mathbb{U}_s(x_t)} \mathop{\mathbb{E}}_{z_{t+1}} \left\{ \overline{J}_{t+1} (f (x_t, u_t, z_{t+1})) \right\} \tag{2-19}$$

$$\mu_t (x_t) \in \operatorname*{argmin}_{u_t \in \mathbb{U}_s(x_t)} \mathop{\mathbb{E}}_{z_{t+1}} \left\{ \overline{J}_{t+1} (f (x_t, u_t, z_{t+1})) \right\}.$$

For each sub-problem, the value function and optimal policy are calculated for states in $\mathbb{X}_s$. When the state $x_{t+1} = f(x_t, u_t, z_{t+1})$ falls outside the discrete subset, i.e. $\mathbb{X} \setminus \mathbb{X}_s$, we use the extension $\overline{J}_{t+1}$ of J_{t+1} via linear interpolation for approximating the value function (see Figure 2-1). [1]

The quantization of the decision space allows us to solve each sub-problem of the DP recursion in Eq. (2-19) by enumerating the allowable decisions $u_t \in \mathbb{U}_s(x_t)$ and choosing the one that minimizes the value function $J_t(x_t)$. If it so happens that more than one allowable action minimizes the value function, we program the algorithm to pick the largest, so that the battery is charged as much as possible during low consumption periods.

At the end of the recursion we are left with an optimal policy in the form of a look-up table $\mu_t : \mathbb{X}_s \to \mathbb{U}_s$ for $t = \{0, 1, \ldots, T-1\}$. That is, for each decision epoch and for each state in the quantized state space the optimal policy gives the best action from the discrete action subset. The control policy can then be used to shave the peak of a load profile. If x_t lands outside the discrete state subset, i.e. $x_t \in \mathbb{X} \setminus \mathbb{X}_s$, the action is calculated by linearly interpolating μ_t (see Figure 2-1):

$$u_t = \overline{\mu}_t(x_t). \tag{2-20}$$

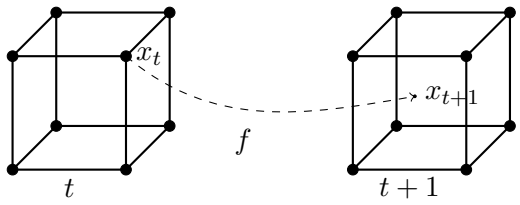

Figure 2-1: Quantization of the state space: at time t the state is limited to a discrete subset; at time t + 1 it is allowed to fall anywhere in the continuous state space. During the recursion, $\overline{J}_{t+1}$ is the linear expansion of J_{t+1}. During control, $\overline{\mu}_t$ is the linear expansion of μ_t.

Algorithm 1 shows the pseudo-code of the DP recursion which receives as input a model of the exogenous information and returns as output the optimal policy.

[1] We note that the notation $\overline{[\cdot]}$ is exclusively used for extension via linear interpolation in this thesis.

Algorithm 1 DP recursion

Input: exogenous information model $\Phi = \{\varphi_t\}_{t=0}^{T-1}$
Output: optimal policy $\{\mu_t\}_{t=0}^{T-1}$

for each state $x_T = (c_T, p_T, d_T) \in \mathbb{X}_s$ **do**
  $J_T(x_T) \leftarrow p_T$
end for

for $t = T-1, \ldots, 0$ **do**
  for each state $x_t = (c_t, p_t, d_t) \in \mathbb{X}_s$ **do**
    for each allowable action $u_t \in \mathbb{U}_s(x_t)$ **do**
      $\nu(u_t) = \underset{z_{t+1}}{\mathbb{E}} \left\{ \overline{J}_{t+1}(f(x_t, u_t, z_{t+1})) \right\}$
    end for
    $J_t(x_t) = \min_{u_t \in \mathbb{U}_s(x_t)} (\nu)$
    $\mu_t(x_t) = \operatorname{argmin}_{u_t \in \mathbb{U}_s(x_t)} (\nu)$
  end for
end for

Chapter 3

Proposed methods

In this section, we begin by laying out the data-driven DP framework, which is the foundation for the two methods. Afterwards, both methods are introduced. At the end of the section, we propose three alterations that can be applied to either method to prevent the occurrence of possible peak increases.

3-1 Data-driven DP

Future demand patterns are unknown in advance, and so is the exact distribution Φ that describes the exogenous information. Hence, we rely on the assumption that historical consumption data from the system to be controlled is available [29].

It has been discussed that the exogenous information is time-varying. Particularly, power consumption profiles exhibit cyclic behaviours [30]:

- intraday cycle, which is the cycle observed on a daily basis;
- intraweek cycle, which is the cycle observed on a weekly basis;
- intrayear cycle, which is the cycle observed on a yearly basis.

These cycles can be seen in Figure 3-1, where the vertical grey lines represent midnight of that day. Consumption is generally higher during day-time hours than night-time, which identifies the intraday cycle. Weekends exhibit different behaviours than weekdays, which identifies the intraweek cycle. Although the figure does not clearly show the intrayear cycle, because the two lines belong to the same year, it is still possible to identify it: the magnitude of consumption is much higher in the winter than in the summer.

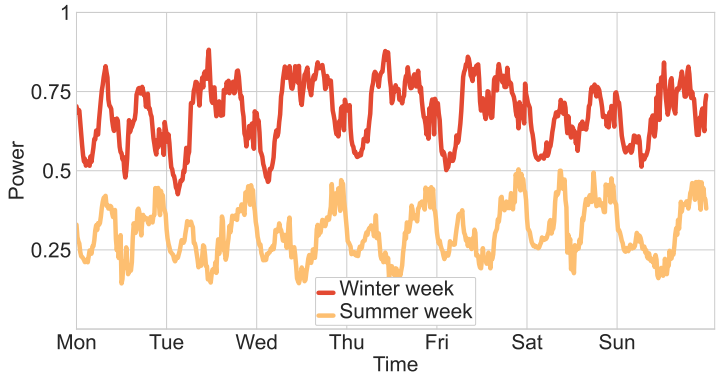

Figure 3-1: Power consumption during the period of one week. in the winter and in the summer.

Because of the intraday cycle, i.e., the daily occurrence of peaks, we consider the horizon T to correspond to a whole day (24 hours). To this end, the historical data is arranged into daily consumption profiles from which we select K profiles that are "relevant" for a target day:

$$\left\{d_t^{(i)}\right\}_{t=0}^{T}, \quad i = 1, \ldots, K. \tag{3-1}$$

The intraweek and intrayear cycles must be taken into consideration when selecting the K relevant profiles to represent a target day.

Although both methods start off from a pool of K profiles and culminate in ways to obtain suitable actions at each decision epoch t, given the state at that time, the basic bedrocks and how each method is applied are fairly distinct: the first method treats data as deterministic paths and calculates the operating policy in real-time, while the second method treats data as stochastic paths and calculates the optimal policy in a one-day-ahead fashion. The CCDDP and SDP methods are described in the two sections below.

3-2 Method 1: CCDDP

The first method is denoted CCDDP, which stands for "convex combination from deterministic DP". As mentioned above, it considers daily demand profiles in the selected pool as deterministic paths. This method requires that, prior to its implementation, a DP optimal policy is determined for each historic profile in the pool using deterministic models for the exogenous information. For each profile in the pool of size K, at time t, the exogenous information z_{t+1} is described by [31]

$$\varphi_t^{(i)} = \delta\left(z_{t+1} - \left(d_{t+1}^{(i)} - d_t^{(i)}\right)\right), \quad i = 1, \ldots, K \tag{3-2}$$

where δ is the Dirac delta and $d_{t+1}^{(i)} - d_t^{(i)}$ is the actual change in demand observed in historic profile i at time t. To point out that the model of the exogenous information treats historical data as deterministic paths, we denote it by $\hat{\Phi}_{\text{det}}^{(i)}$. For each daily profile in the pool, we solve

the DP recursion in Algorithm 1 with input $\hat{\Phi}^{(i)}_{\text{det}} = \left\{\varphi^{(i)}_t\right\}^{T-1}_{t=0}$ and output $\mu^{(i)} = \left\{\mu^{(i)}_t\right\}^{T-1}_{t=0}$. Note that the expectation in Eq. (2-19) can be rewritten as

$$\mathbb{E}\left\{\overline{J}_{t+1}\left(f\left(x_t, u_t, z_{t+1}\right)\right)\right\} = \overline{J}_{t+1}\left(f\left(x_t, u_t, d^{(i)}_{t+1} - d^{(i)}_t\right)\right). \tag{3-3}$$

Provided that these deterministic optimal policies are available, the CCDDP method calculates the operating policy in real-time via a convex combination of them, that is,

$$\mu_t = \sum_{i=1}^{k} \alpha^{(i)}_t \mu^{(i)}_t \tag{3-4}$$

where $\alpha^{(i)}_t$ is the coefficient of the convex combination assigned to the i-th historic profile in the pool, at time t. At each time step t, the coefficient corresponding to the i-th policy may change, hence it is denoted $\alpha^{(i)}_t$. In order to determine the appropriate coefficients, we consider the most recently observed W demand values of the target day, $w_t = \{d_{t'}\}^t_{t'=t-W+1}$, i.e., the "window" of length W of most recent observed demand values. Furthermore, we also consider the equivalent windows in the historic profiles, which we denote $w^{(i)}_t = \{d^{(i)}_{t'}\}^t_{t'=t-W+1}$. The coefficients $\alpha^{(i)}_t$ assigned to each profile i in the pool at time t then depend on how "similar" the window $w^{(i)}_t$ is to target window w_t. The pseudo code of the CCDDP method is shown in Algorithm 2. In what follows we provide two methods for determining the coefficients $\alpha^{(i)}_t$ in the convex combination:

- Least squares optimization:
  We formulate the least squares problem to obtain the coefficients of a convex combination $\alpha^{(i)}_t$ as follows:

$$\begin{aligned} \min_{\alpha_t} \quad & \|Q_t\alpha_t - w_t\|_2^2 \\ \text{s.t.} \quad & \sum_{i=1}^{m} \alpha^{(i)}_t = 1 \\ & \alpha_{i,t} \geq 0 \end{aligned} \tag{3-5}$$

  where $Q_t \in \mathbb{R}^{W\times K}$ with the sub-profiles $w^{(i)}_t$ from the historical data as its columns, and α_t is a column vector of length K containing $\alpha^{(i)}_t$. The constraints ensure that the coefficients obtained will form a convex combination, i.e., they must be non-negative and sum to 1.

- p-norm based coefficients:
  For each profile i in the pool of historical data, at each time step t, we define the distance between w_t and $w^{(i)}_t$

$$\delta^{(i)}_{p,t} = \|w_t - w^{(i)}_t\|_p \tag{3-6}$$

  where $\|a\|_p$ is the p-norm of the vector $a \in \mathbb{R}^n$. The more similar a historical sub-profile $w^{(i)}_t$ is to w_t, the smaller the p-norm will be. Hence, we define

$$\gamma^{(i)}_t = \frac{1}{\delta^{(i)}_{p,t}} \tag{3-7}$$

as the similarity measure and take the convex coefficients $\alpha_t^{(i)}$ to be the normalized $\gamma_t^{(i)}$, i.e.,

$$\alpha_t^{(i)} = \frac{\gamma_t^{(i)}}{\sum_{j=1}^{k} \gamma_t^{(j)}}. \tag{3-8}$$

Algorithm 2 CCDDP

Input: pool of K historic demand profiles
deterministic optimal policies $\mu^{(i)}$
width of moving window W
current time t and current state x_t
most recent demand values (target sub-profile) w_t
Output: CCDDP operation input u_t

for each day i in the pool of size K **do**
$w_t^{(i)} \leftarrow$ time window of width W ending at time t belonging to day i
$\alpha_t^{(i)} \leftarrow$ coefficient assigned to day i in the pool, based on how "similar" $w_t^{(i)}$ is to w_t
end for
$\mu_t = \sum_{i=1}^{k} \alpha_t^{(i)} \mu_t^{(i)} \rightarrow u_t = \overline{\mu}_t(x_t)$

3-3 Method 2: SDP

The acronym SDP stands for "stochastic DP". In this method, the historical daily demand profiles in the pool of size K are taken to be stochastic paths. These paths are combined to build a single stochastic model of the exogenous information for a particular target day. To this end, we consider the exogenous information to be not only time-dependent but also state-dependent. For instance, if demand is already high in the morning it is unlikely that it will increase much more. In order to construct the stochastic model of the exogenous information, we quantize the outcome space into N_z discrete points as follows:

$$\mathbb{Z}_s = \left\{ z^{\min} + \frac{j \cdot \left(z^{\max} - z^{\min}\right)}{N_z - 1},\ \ j = 0, \ldots, N_z - 1 \right\}. \tag{3-9}$$

This allows us to build the model as a set of T probability matrices of size $N_d \times N_z$, with the t-th matrix containing a probabilistic model of the exogenous information for time t. The t-th matrix is defined as [1]:

$$[\varphi_t]_{row,col} = \mathbb{P}\left(z_{t+1} = z | t, d_t = d\right) \tag{3-10}$$

with

$$(d, z) = \left(\frac{row}{N_d - 1} \cdot d^{\max},\ \ z^{\min} + \frac{col \cdot \left(z^{\max} - z^{\min}\right)}{N_z - 1} \right) \in \mathbb{D}_s \times \mathbb{Z}_s. \tag{3-11}$$

[1] Throughout this work, the convention used is that the indexing of rows and columns starts from 0, i.e., $row \in \{0, 1, \ldots, N_d - 1\}$ and $col \in \{0, 1, \ldots, N_z - 1\}$.

We describe the procedure to obtain the stochastic model of z_{t+1} below. It is outlined for a single time step t and should be repeated for all $t = 0, \ldots, T-1$. Let us begin by introducing two useful operations. Consider the interval $\mathbb{A} = [a^{\min}, a^{\max}] \subset \mathbb{R}$ and its discretization

$$\mathbb{A}_s = \left\{ a^{\min} + \frac{j \cdot (a^{\max} - a^{\min})}{N_a - 1}, \;\; j = 0, \ldots, N_a - 1 \right\}. \tag{3-12}$$

For any $a \in \mathbb{A}$, we define

$$\Pi_{\mathbb{A}_s}(a) = \underset{\tilde{a} \in \mathbb{A}_s}{\operatorname{argmin}} |a - \tilde{a}| \tag{3-13}$$

to be the projection of a on $\mathbb{A}_s$, that is, the closest point to a in $\mathbb{A}_s$. Moreover, for any $a \in \mathbb{A}_s$, we define its corresponding index by

$$\Gamma_{\mathbb{A}_s}(a) = \frac{a - a^{\min}}{a^{\max} - a^{\min}} (N_a - 1). \tag{3-14}$$

For each historic profile $\left\{ d_t^{(i)} \right\}$, $i = 1, \ldots, K$, at each time t, an auxiliary matrix $A_t^{(i)}$ of size $N_d \times N_z$ is initialized with zero values. The projections $\Pi_{\mathbb{D}_s}\left(d_t^{(i)}\right)$ and $\Pi_{\mathbb{Z}_s}\left(z_{t+1}^{(i)} = d_{t+1}^{(i)} - d_t^{(i)}\right)$ are calculated as in Eq. (3-13) and the respective pair $\left(\Gamma_{\mathbb{D}_s}\left(d_t^{(i)}\right), \Gamma_{\mathbb{Z}_s}\left(d_{t+1}^{(i)} - d_t^{(i)}\right)\right)$, i.e., the indexes of the projections, is determined from Eq. (3-14). The value in $A_t^{(i)}$ corresponding to the pair $\left(\Gamma_{\mathbb{D}_s}\left(d_t^{(i)}\right), \Gamma_{\mathbb{Z}_s}\left(d_{t+1}^{(i)} - d_t^{(i)}\right)\right)$ is given the value 1, and a small value ϵ is added to all the elements in that row. The matrices $A_t^{(i)}$ have the characteristic that all but one row is full of zeros.

Once all matrices $A_t^{(i)}$ are determined, they are combined into a single matrix

$$A_t = \sum_{i=1}^{K} A_t^{(i)} \tag{3-15}$$

It might happen that some rows in the matrix A_t are zero. In such case, these rows are be filled by combining the non-zero rows, weighted by how close they are to the zero row. This is done under the assumption that the missing information will behave somewhat similar to a combination of the available information. Each non-zero row, indexed r, contributes with a weight

$$\alpha^r = \frac{1}{|row - r|}, \;\; r \in \{0, \ldots, N_d - 1\} \setminus row. \tag{3-16}$$

In order to avoid that previously zero rows that have now been filled will contribute to another zero row, we introduce the matrix φ_t, equal to the matrix A_t. The zero rows in φ_t are filled according to

$$\varphi_t(row, col) = \sum_{r \in \{0, \ldots, N_d - 1\} \setminus row} \alpha^r A_t(r, col), \;\; col = 0, \ldots, N_z - 1. \tag{3-17}$$

To guarantee that the upper and lower limits of the demand variable are satisfied, we must ensure that any matrix elements that lead to a future demand d_{t+1} beyond those limits have a zero probability of occurrence. Any probability assigned to one of these elements in the early stages of the process must be removed from such entry and added to the closest possible

event. For example, for $d_t = 0.2$, the occurrence $z_{t+1} = -0.3$ would lead to a negative future demand. The probability assigned to $z = -0.3$ should be added to the probability of the first value of $z_{t+1} \in \mathbb{Z}_s$ that yields a non-negative future demand, which would have to be greater than or equal to -0.2. Finally, all rows of φ_t should be normalized, such that each row sums to 1. This procedure is outlined in more detail in Algorithm 5 which can be found in Appendix A.

Once a model $\hat{\Phi}_{\text{stoch}} = \{\varphi_t\}_{t=0}^{T-1}$ is available, an operating policy is obtained from the DP recursion in Algorithm 1, with input $\hat{\Phi}_{\text{stoch}} = \{\varphi_t\}_{t=0}^{T-1}$ and output $\mu = \{\mu_t\}_{t=0}^{T-1}$. Note that the quantization of the random variable allows to re-write the expectation in Eq. (2-19) as

$$\mathop{\mathbb{E}}_{z_{t+1}} \{J_{t+1}(f(x_t, u_t, z_{t+1}))\} = \sum_{n=0}^{N_z-1} P_n \overline{J}_{t+1}(f(x_t, u_t, z_n)) \tag{3-18}$$

where

$$z_n = z^{\min} + \frac{n\left(z^{\max} - z^{\min}\right)}{N_z - 1} \in \mathbb{Z}_s \tag{3-19}$$

and P_n is the probability of occurrence of z_n given by $[\varphi_t]_{r,n}$ with r given by the projection of d_t onto $\mathbb{D}_s$, as in equation Eq. (3-13).

The SDP policy is obtained in a one-day-ahead fashion, i.e., the DP recursion is ran once, before the target day, and defines the operating plan for the full day ahead. Then, at each time t in the target day, given the current state x_t, this policy is queried to give the best action:

$$u_t = \overline{\mu}_t(x_t) \tag{3-20}$$

Recall that $\overline{\mu}_t$ is the linear expansion of the SDP policy μ_t.

3-4 Preventing peak increases

As will become evident in Chapter 4, both methods are unsuccessful at guaranteeing peak shaving for all daily demand profiles, in some cases even leading to peak increases. Hence, we propose three alterations that can be applied to both CCDDP and SDP methods to prevent the occurrence of peak increases. Each of the proposed alterations is applied to either method at control time.

3-4-1 ε-alteration

Given the current state x_t, a policy gives the action u_t we should take by querying $\overline{\mu}_t(x_t)$. In order to get a more conservative action from the policy, we propose to subtract a small value ε from the peak p_t, that is, to query the policy μ_t at $x'_t = (c_t, p_t - \varepsilon, d_t)$. See Algorithm 3 below for a better understanding.

Algorithm 3 ε-alteration

Input: current state x_t
operating policy μ_t obtained from either CCDDP or SDP
parameter ε
Output: modified action u'_t

$x'_t \leftarrow$ modified position of the system at time t of the target day: $x'_t = (c_t, p_t - \varepsilon, d_t)$
$u'_t \leftarrow$ modified action suggested by the operating policy given $x'_t : u'_t = \overline{\mu}_t(x'_t)$

3-4-2 $\hat{z}$-alteration

This alteration requires making an estimate of the next exogenous information which is represented by $\hat{z}_{t+1}$. Given this estimate, the decision u_t retrieved from either CCDDP or SDP policy and the current demand d_t, we calculate the expected peak at $t+1$ as $\hat{p}_{t+1} = d_t + \hat{z}_{t+1} + u_t$. If the action is a charging command that leads to $\hat{p}_{t+1} > p_t$ then we will rather not act on the battery, i.e., u_t will be replaced with value 0. For the CCDDP method the estimated demand change is calculated as:

$$\hat{z}_{t+1} = \sum_{i=1}^{K} \alpha_t^{(i)} \left(d_{t+1}^{(i)} - d_t^{(i)} \right) \tag{3-21}$$

and for the SDP method as:

$$\hat{z}_{t+1} = \sum_{i=1}^{K} \frac{1}{K} \left(d_{t+1}^{(i)} - d_t^{(i)} \right). \tag{3-22}$$

3-4-3 $z^{\max}$-alteration

This alteration is a "worst-case scenario" version of Section 3-4-2. Instead of using an estimate $\hat{z}_{t+1}$, it takes a more conservative approach: it uses the maximum value of change in demand seen in historical data.

The algorithm below shows the pseudo-code behind the $\hat{z}$- and $z^{\max}$-alterations.

Algorithm 4 $\hat{z}_{t+1}$- and $z^{\max}$- alterations

Input: current state x_t
operating policy μ_t obtained from either CCDDP or SDP
estimate of demand change, $\hat{z}_{t+1}$ or $z^{\max}$
Output: modified action u'_t

$u_t \leftarrow$ action suggested by the operating policy given the current state x_t: $u_t = \overline{\mu}_t(x_t)$
if $d_t + (\hat{z}_{t+1}$ or $z^{\max}) + u_t > p_t$ **and** $u_t > 0$ **then**
  $u'_t = 0$
end if

Chapter 4

Simulation results

The two proposed methods will be tested against a real set of electricity consumption data. The performance of the proposed methods will be evaluated based on how much they are able to shave the peak of a daily demand profile. To this end, we define the peak shaving percentage achieved for a profile with T time steps as

$$ps_T = \frac{d_T^{\max} - p_T}{d_T^{\max}} \times 100\% \tag{4-1}$$

where $d_T^{\max}$ is the maximum demand observed during that period and p_T is the peak load after shaving at the end of the period.

All simulations shown in this section were performed for the the quantization of the continuous variables featured in Table 4-1, unless clearly stated otherwise.

Table 4-1: Number of quantization points of each state, decision and random variable.

N_c	N_p	N_d	N_u	N_z
5	11	11	11	21

Unless stated otherwise, the methods were simulated for every daily profile in the data set. In all simulations, the state of the system is initialized as follows:

- demand d_0: it is initialized with the first demand value observed from data for a particular target day;
- peak p_0: is is initialized with the same value as the demand;
- SoC c_0: is initialized with value 0.3.

The peak is initialized equal to the demand because we simulate each profile individually and do not consider continuation of time. Hence, the peak starts out as the largest (and only) demand value seen so far. Initializing the battery with different SoC does not produce

significant changes in the results due to the general shape of the test data, therefore, 0.3 was chosen as an arbitrary value that is neither fully charged nor fully discharged.

The remaining of this section is organized as follows: Section 4-1 presents some aspects of the real data set used in the simulations. Section 4-2 shows an example of how peak shaving is carried out for a daily profile in the data set, using the SDP method. Section 4-3 presents the results of the CCDDP method simulations and Section 4-4 shows the simulation results of the SDP method. Section 4-5 assesses the optimality of the two proposed methods based on simulations performed on artificial demand profiles. In Section 4-6, the three proposed alterations to improve the reliability of the methods are introduced in the simulations, and the results are discussed.

It is be interesting to see the distribution of peak shaving percentages achieved for all profiles in the data set when full knowledge of the exogenous information is assumed (shown in Appendix C), as it gives an idea of the best peak shaving performance we can expect given the quantization points in Table 4-1.

4-1 Data set

The data set contains the power demand values observed throughout the year 2018 with measurements taken every 15 minutes. Appendix B shows the normalized demand profiles throughout the entire year. The first data point corresponds to 00:00 (midnight) January 1st, 2018 and the last corresponds to 23:45 December 31st, 2018. The first decision of the day is made at 00:00 and the last decision at 23:45. The terminal step is the midnight of the following day. Hence, the decision epochs are $t = 0, 1, \ldots, T-1$ for $T = 96$.

Table 4-2 shows the data and battery parameters used in the subsequent simulations. The data parameters were retrieved from the data set directly, and the battery parameters were provided along with the data set. The data set is private, therefore all parameters in the table are normalized by the maximum value of demand observed.

Table 4-2: Data and battery parameters.

$d^{\max}$	$z^{\min}$	$z^{\max}$	$u^{\min}$	$u^{\max}$	$\overline{\alpha}$	$\underline{\alpha}$
1	-0.182	0.273	-0.273	0.273	0.965	0.871

Due to the lack of real demand data over multiple years, the available data set will be used in a circular fashion, i.e. we assume that the day after December 31st, 2018 is January 1st, 2018.

4-2 Illustrative example

We show an illustrative example of how the SDP method performs for a particular target day in Figure 4-1. Figure 4-1a shows the consumer demand profile, the load seen by the grid and the peak evolution throughout the target day, Figure 4-1b shows the SoC evolution throughout the day and Figure 4-1c shows the sequence of decisions taken at every time

step of the day. The peak shaving percentage is calculated from Eq. (4-1) where $d_T^{\max}$ is the maximum value of the red line and p_T is the final value of the blue line. For this example, the peak is shaved by 13.0294%.

The behaviour displayed meets the expectations. Recall that the peak is initialized with the same value as the initial demand. Then, in the first hours of the day when demand is still decreasing the battery recharges from midnight until around 5AM. The decisions are positive, the SoC rises and the load seen by the grid is higher than the consumer demand. This behaviour is observed again right after the first peak which occurs between 5AM and 7AM. During the peaks, battery supplies some of its stored energy to the consumer: it receives negative inputs, hence the SoC decreases and the load curve stays below the demand curve.

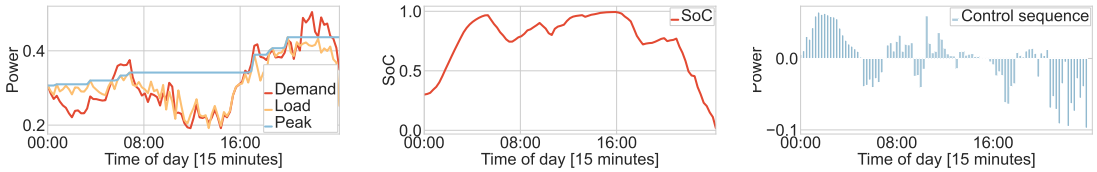

(a) (b) (c)

Figure 4-1: SDP method is applied to July 27: (a) consumer demand, load seen by the grid and peak; (b) state-of-charge; (c) sequence of decisions.

4-3 CCDDP simulation results

In the CCDDP method, weights $\alpha_t^{(i)}$ are assigned at each time step to the daily demand profiles in a pool of K relevant profiles. This is done by considering the most recent W demand values as well as the equivalent windows from the profiles in the pool. The deterministic optimal policies at time t corresponding to profile i contribute to the control policy for a given target day with weight $\alpha_t^{(i)}$.

In the simulations below, the pool of historic profiles chosen to represent any target profile is composed of all remaining profiles in the data set. Furthermore, the length of the sub-profiles was taken to be $W = 16$, i.e., the most recent 4 hours. A short analysis of the effect of varying these parameters is provided in Appendix D

Four different simulations of the CCDDP method were performed, with respect to how the coefficients of the convex combination, $\alpha_t^{(i)}$, are obtained: the least squares optimization in Eq. (3-5) and the p-norm based coefficients from Eq. (3-6), Eq. (3-7) and Eq. (3-8), with $p \in \{1, 2, \infty\}$ [1].

The CCDDP method was simulated for every daily profile in the real data set under the conditions mentioned above. The results are shown in Figure 4-2.

[1] Recall that, for $a \in \mathbb{R}^n$ we have:

$$\|a\|_1 = \sum_{j=1}^{n} |a_j|,$$

$$\|a\|_2 = \sqrt{\sum_{j=1}^{n} (a_j)^2},$$

$$\|a\|_\infty = \max_j |x_j|.$$

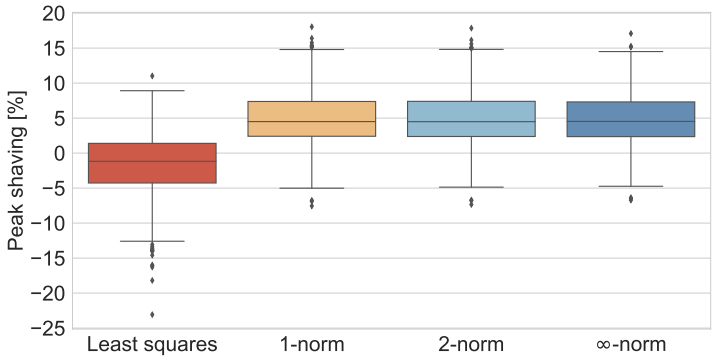

Figure 4-2: Peak shaving results of the CCDDP method.

The CCDDP method with coefficients obtained from least squares clearly shows the worst performance, while among the p-norm variations there is not a significant distinction between the results.

The least squares method attempts to find the coefficients $\alpha_t^{(i)}$ such that a convex combination of the data in the matrix Q_t approximates the target sub-profile w_t with minimized error. This method tends to perform well if the data observations follow a Gaussian distribution [32]. For this problem, this is not necessarily the case, because we use $K = 364$, whatever the target day is, there are many sub-profile in the matrix Q_t that are far off from the target sub-profile (see Figure 3-1).

On the other hand, the p-norm based coefficients are calculated such that they are inversely proportional to the p-norm distance between each sub-profile $w_t^{(i)}$ in the data and the target sub-profile. Hence, they are directly related to the actual observed distance between the sub-profiles and do not make any assumptions regarding the nature of the distribution. The results obtained from the p-norm metrics are very similar for all values of p. This suggests that, even though the p-norm metrics may differ significantly for each p, once the distances are inverted and normalized to obtain the coefficients, they become insignificant. This speculation is supported by observations which can be found in Appendix E.

4-4 SDP simulation results

To simulate the SDP method on a target profile, the pool of relevant data is composed of the K demand profiles of the days immediately prior to the target day, for $K = \{10, 60, 364\}$. As mentioned above, the data set is used in a circular fashion, therefore, when this method is applied to January 1st 2018, for example, we consider that the K days prior to the target day are the last K days of the year 2018.

The method is simulated for every daily demand profile in the data set. The peak shaving results are shown in Figure 4-3 for each value of K.

The results obtained for $K = 10$ are spread over a wider range of peak shaving percentages compared to the other simulations, and the median peak shaving achieved is the lowest

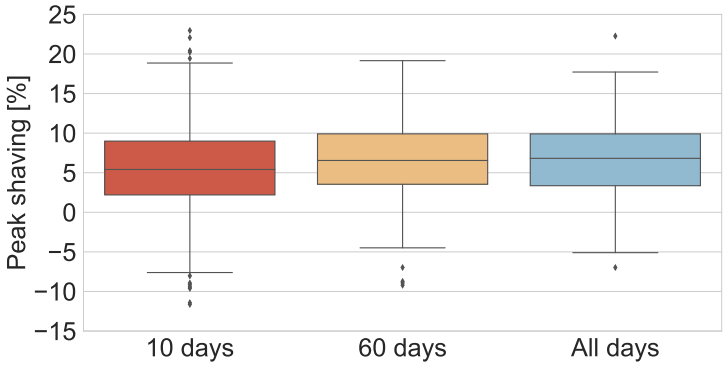

Figure 4-3: Peak shaving results of the SDP method.

observed over the three simulations. This suggests that, although for a few outlier cases using 10 previous days to model the exogenous information give very good results, the minimum value of this box is below the minimum values of the remaining boxes, with another few outliers even lower. The middle and right-most boxes show a slight improvement relative to the 10-days box. Although the 60-days box shows a few outliers on the negative side, its maximum line is well above that of the 364-days box (the positive outlier is not considered as the maximum of the right-most box). The 60 days prior to a target day comprise much more information than just the 10-days, making the random variable model more robust to unpredictable behaviour of the target day. This robustness is also observed on the right-most box. Although using information from an entire year before the target day inevitably includes demand shapes that are very different from the target day, this is balanced out because we are also including more demand shapes that contribute to a more accurate representation of the target day. For instance, for the target day July 27th there are relevant profiles before, as well as after, the target day. Using 60 previous days only takes into account the relevant profiles that happened before the target day, while using all remaining days in the data includes the profiles that happened after.

4-5 Test with artificial data

In order to determine how sub-optimal our solutions are, both methods were tested on artificial demand profiles. To generate these profiles, we selected one of the stochastic models of the exogenous information used throughout this work. Particularly, the chosen model is the one obtained from applying Algorithm 5 to the pool composed of 60 demand profiles prior to July 27th. For the purpose of these tests, this model is taken to be a true distribution of the exogenous information, Φ_{stoch}. The DP recursion is run and we obtain an optimal policy $\{\mu_t^*\}_{t=0}^{T-1}$ and a value function $\{J_t^*\}_{t=0}^{T}$. For some initial condition x_0, the optimal expected cost, which, in the scope of this work, is equivalent to the optimal expected peak, is given by $J_0^*(x_0)$. From this model, two sets of artificial demand profiles are generated: a train set with N profiles and a test set with $100 \times N$ profiles. All artificial profiles are generated starting from the same initial state, where the SoC is 0.3 and the peak and demand are the initial demand of July 27th which, normalized by the maximum demand observed in the private

data, is 0.3066.

Each method was tested on three different settings:

1. train set size $N = 60$, test set size $100 \times N = 6000$; grid size from Table 4-1;
2. train set size $N = 60$, test set size $100 \times N = 6000$; finer grid quantization (grid size G4 from Table 5-1);
3. train set size $N = 100$, test set size $100 \times N = 10000$; grid size from Table 4-1.

To evaluate the CCDDP method, we generate deterministic models of the exogenous information for each profile in the train set, as in equation Eq. (3-2) and run the DP recursion to obtain a deterministic optimal policy for each of these profiles. Then, the CCDDP method in Algorithm 2 is applied for each profile in the test set, at each time step. To evaluate the SDP method, an approximation of the true distribution is computed from the train set via Algorithm 5, and we denote it $\hat{\Phi}_{\text{stoch}}$. The DP recursion is run for this approximation and the resulting policy $\{\hat{\mu}_t\}_{t=0}^{T-1}$ is applied to every profile in the test set.

Figure 4-4 is split into three pairs of box plots, corresponding to the three test settings. Each pair contains a red box, which shows the distribution of the SDP peaks after shaving, and a yellow box for the distribution of the peaks after shaving obtained with CCDDP, for that setting. Each box contains a horizontal grey line representing the median of the observations, and a white circle representing the mean. For each setting, we also calculate the expected optimal peak, given by $J_0^*(x_0)$, which is represented by the full black horizontal lines. Furthermore, the optimal policy μ^* obtained for each setting is applied to the appropriate test set. The mean and median of peaks achieved with μ^* are also shown in the figure by the dashed and dotted horizontal lines, respectively.

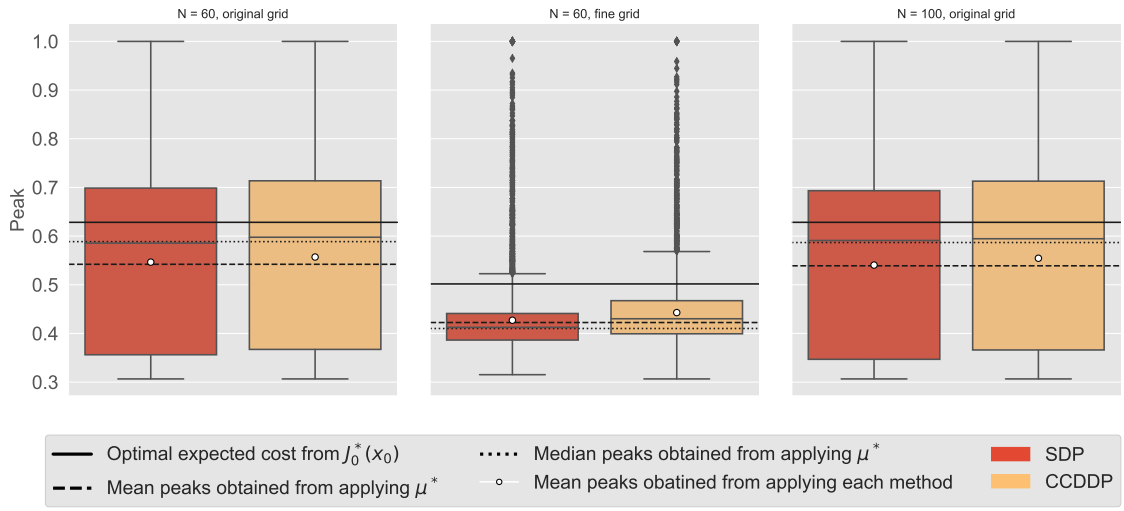

Figure 4-4: Testing CCDDP method and SDP method on artificial data, under three different settings.

Immediately, we see that the distribution of peaks after shaving obtained from using either method is quite similar, for these artificial profiles, particularly for the gross grid. It is also immediate to conclude that the finer grid significantly improves the performance of either method.

Throughout all three test settings we observe that the optimal expected peak calculated from the value function at the initial condition is higher than both the median and mean of peaks achieved for either method, suggesting that both methods are above optimal operation, which is unexpected. However, the dashed black lines always stay below the white circles. Similarly, the dotted lines stay below the grey lines of each box (except for the left-most red box, in which the dotted line is slightly above the median). The distances of the dashed lines to the white circles and of the dotted lines to the median lines are very small, and it becomes even smaller for larger N.

The proximity between the dashed lines and white circles, as well as that of the dotted lines to the median grey lines, suggests that both methods are sub-optimal, but their performance is very close to the optimal solutions. The observation that the expected optimal peak is higher than the remaining solutions seems to suggest that the computational errors are more significant in the estimation of the value function than in the estimation of the optimal policy.

4-6 Results of preventing peak increases

As seen in the past two sections, even when the proposed methods perform their best they still, occasionally, generate peak increases. Each of the three proposed alterations (ε-alteration, $\hat{z}$-alteration and $z^{\max}$-alteration) was applied to both the 2-norm variation of CCDDP method and the 60 days variation of SDP method. The results of how each alteration affects these two methods are shown in Figure 4-5a and Figure 4-5b, respectively. The figures show two different quantities: the change in peak shaving percentage that each of the alterations produces for each target day as well as the actual peak shaving percentages achieved for each target day after applying the alterations. The former is defined as the difference between *ps* obtained with the modified methods and the *ps* achieved with the plain methods. In these simulations, ε was taken to be 0.1.

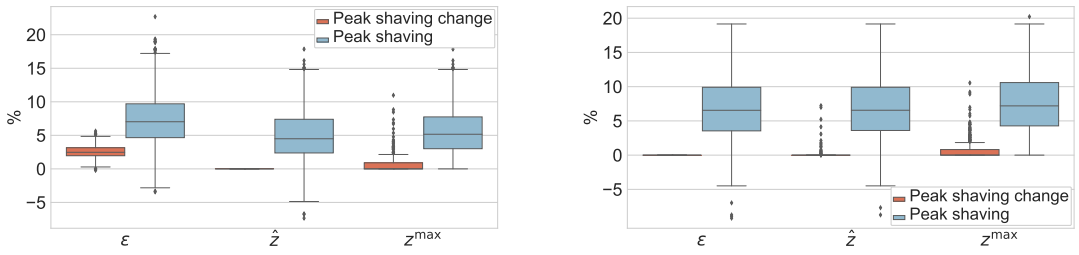

Figure 4-5: Effect of ε-, $\hat{z}_{t+1}$- and -$z^{\max}$- alterations on: (a) CCDDP method using 2-norm to calculate coefficients; (b) SDP method using 60 preceding days.

For the CCDDP method, the ε-alteration queries a policy that is a combination of other optimal policies that were calculated for exactly known profiles. Hence, the ε-alteration

allows to take more conservative actions. As seen in Figure 4-5a, overall, it helps to raise the peak shaving percentages. However, there are still some peak increases observed. For the SDP method, this alteration does not produce any changes.

From the figures we immediately conclude that the $\hat{z}$-variation is not helpful in preventing the occurrence of peak increases: for the most part it has no impact with the exception of a few outliers. For the CCDDP it does not change anything for any day. This is because the demand variation is implicitly coded in the optimal policies obtained by both methods. In the SDP it is encoded in the model of the exogenous information z_{t+1} and in CCDDP it is encoded in deterministic optimal policies of the profiles in the database and the weights assigned to each of them.

The $z^{\max}$-alteration is the most conservative approach, as it assumes a worst-case scenario in demand variation, i.e., assuming that the demand variation will be the worst possible, it takes the safest possible action. This alteration produces the desired result of eliminating the occurrence of peak increases for both methods with an insignificant compromise of the median and maximum peak shaving results.

Chapter 5

Final remarks

In this section, we perform an analysis on important features of the peak shaving methods proposed in this work. In Section 5-1, we discuss two particular limitations of the methods and how they influence the peak shaving results. In Section 5-2, we analyse the computing times of both proposed methods and how these vary for different quantization grid sizes. The peak shaving sensitivity to the grid sizes is also shown for two particular daily demand profiles from the real data set used throughout the work. In Section 5-3, a summary of this work and final conclusions are presented, as well as some future work suggestions to further improve the methods.

5-1 Limitations of the methods

Peak shaving applications commonly exhibit two limitations [21, 16, 19]. These are: (1) shaving peaks with long duration and (2) historical data not being a good representative of the target profiles. The first limitation is directly related to the battery integrated in the system, as shaving of long peaks is primarily constrained by its capacity. The second limitation is a product of relying on available historical data.

Figure 5-1 shows the average daily profile in the year, a demand profile from a summer day and another from a winter day. As already shown in Figure 3-1, electricity consumption is higher in the winter than in the summer. The figure below shows that the average profile is closer to the summer profiles, both in shape and in magnitude. Furthermore, the peak in the winter profile is "longer" than that of the summer profile. We will discuss peak duration below, under paragraph "Quantifying peak duration".

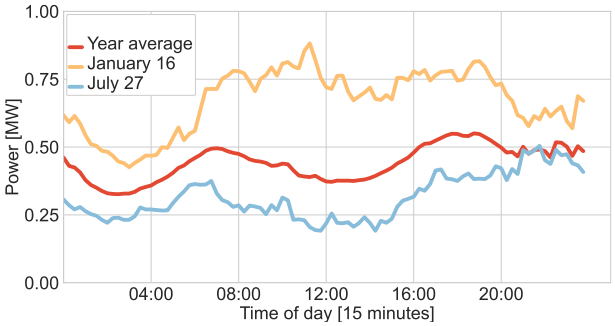

Figure 5-1: Average profile in 2018, winter profile (January 16th) and summer profile (July 27th).

In order to assess if the proposed methods are also influenced by the duration of the peaks to be shaved, the peak shaving percentages achieved for each day in the year were plotted on a calendar, as seen in Figure 5-2, where Figure 5-2a shows the peak shaving performance of the CCDDP method and Figure 5-2b for the SDP method.

In both figures, a pattern can be identified, which is that peak shaving is, generally, more successful in the months between April and August and lower throughout the remaining of the year.

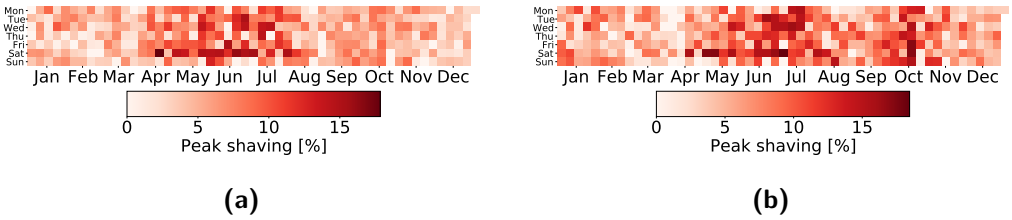

Figure 5-2: Peak shaving values for each day in 2018 shown on a calendar (a) obtained with the CCDDP method with convex coefficients calculated from 2-norm and $z^{\max}$-alteration and (b) obtained with the SDP method using the 60 previous days to model the random variable and $z^{\max}$-alteration.

In order to properly evaluate how both limitations hold for the proposed methods, let us define ways of quantifying peak duration as well as the similarity between a daily profile and a pool of "relevant" historical data.

Quantifying peak duration For a given daily demand profile, the peak duration is the number of the consecutive time steps during which the demand is above the horizontal line located at 90% of the peak demand of that day. If there is more than one instance where this occurs, we consider the longest period to be the peak duration.

Quantifying similarity Similarity encodes how well the pool of historical data represents the target day. For a given target demand profile there is a pool of relevant historical data of size K (e.g. previous K=60 days). We quantify similarity by first determining the Euclidean

distances between the target profile and each profile in the pool, $\delta^{(i)}$, and then calculating the average Euclidean distance

$$\overline{\delta} = \sum_{i=1}^{K} \frac{1}{K} \delta^{(i)}. \tag{5-1}$$

Given these measures of peak duration and similarity we plot the peak shaving results of each day against the duration of the longest peak of day and the similarity between the pool of historical data and that day. Figure 5-3 relates the peak shaving results attained from the CCDDP method (Figure 5-3a) and from the SDP method (Figure 5-3b).

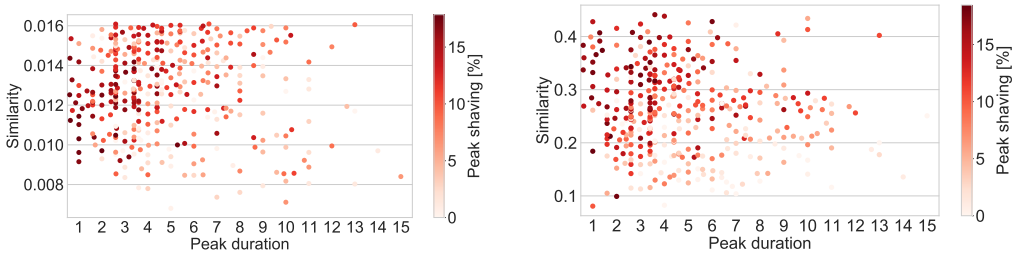

Figure 5-3: Effect of peak duration and representativity in peak shaving performance: (a) CCDDP, 2-norm based coefficients, modified with $z^{\max}$; (b) the SDP method, 60 preceding days, modified with $z^{\max}$.

In both figures it becomes clear that the duration of the peak to be shaved is an important factor for the performance of peak shaving. The circles are darker for lower values of peak duration and become lighter as the peak duration increases.

Regarding similarity, in Figure 5-3a it is possible to see that, in general, the circles have darker shades for higher values of similarity and lighter shades for lower similarities. When analysing Figure 5-3b, however, we note that the effect of similarity is more significant in the SDP method rather than in the CCDDP method. The similarity measure considered assigns the same weight to all K profiles in the pool. For the SDP method it is composed of the 60 profiles prior to the target day, which are the profiles used to derive the model of the exogenous information. Hence it is natural that similarity plays a significant role in the performance of peak shaving. For the CCDDP method, the pool is composed of all the profiles in the year except the target day. This similarity measure assigns uniform weights to each profile to quantify how well the pool represents the target day. Naturally, the average of the year does not represent any single day accurately. However, note that it is closer to summer profiles than to winter profiles, as seen in Figure 5-1. In the CCDDP method, the weights assigned to each historic profile are adapted at each time step. In other words, the method adapts these weights in such a way that the pool of historic profiles best represents the target day, hence allowing to achieve satisfactory peak shaving performances, regardless of how well the pool represents the target day when all of its profiles are given the same importance. Chapter F shows the effect of peak duration and similarity to the historic pool for the CCDDP method if a different similarity measure is used.

5-2 Performance with respect to grid size

In order to better understand how the performance of each method changes with the grid size, a short sensitivity and running time analysis was carried out. Each method is evaluated on the following three metrics:

1. peak shaving performance;
2. recursion time —the time it takes to calculate one optimal policy from the DP recursion;
3. control time —the time it takes to calculate an optimal action in real time; for the SDP method, this corresponds to the time it takes to query the optimal policy at the current state, i.e. $\overline{\mu}_t(x_t)$; for the CCDDP method, this corresponds to the time it takes to obtain the coefficients of the convex combination, combining the deterministic optimal policies and querying the resulting control policy, at each time t.

The simulations featured in this analysis were run on MATLAB® on a laptop with Windows 10 OS x64, 8,00GB RAM and a processor with the following characteristics: Intel(R) Core(TM) i5-1035G1 CPU @ 1.00GHz - 1.19GHz. It was observed that, when running the two methods in Python code on the same laptop, the computation times were significantly higher.

Each method was evaluated for the grid sizes introduced in Table 5-1. This table shows the number of points used to quantize each variable, as well as the total points at which the value function is evaluated for one time step of the DP recursion. The CCDDP method considers the random variable to be continuous and with a Dirac delta distribution, hence, the total number of evaluation points is given by $N_c \times N_p \times N_d \times N_u$. In the SDP method, the outcome space is also quantized, and the total number of points is given by $N_c \times N_p \times N_d \times N_u \times N_z$. Therefore, the total number of evaluation points involved in the CCDDP method is smaller than that involved in the SDP method.

Table 5-1: Grid sizes used in the sensitivity analysis.

	Variables' number of points					Total number of evaluation points	
	N_c	N_p	N_d	N_u	N_z	CCDDP	SDP
G1	5	5	5	11	11	1 375	15 125
G2	5	11	11	11	11	6 655	73 205
G3	5	11	11	11	21	6 655	139 755
G4	7	15	15	15	25	23 625	590 625
G5	11	21	21	21	31	101 871	3 158 001

In order to evaluate the CCDDP method on a particular day for each grid size, it is required that a deterministic optimal policy is available for each daily profile in the historical profiles pool. Calculating one year's worth of deterministic optimal policies for each grid in Table 5-1 would not be feasible in a reasonable amount of time. For this reason, the CCDDP method is evaluated for three of the grids in the table: G1, which is the grossest, G3, which is the grid used throughout the work, and G4. G4 was chosen over G5 as it contains significantly fewer evaluation points than the latter. In order to evaluate the SDP method on a particular day for each grid size, it is necessary that a probabilistic model of the random variable for

that day and size is available, such that the stochastic DP recursion can calculate an optimal policy. This means that, in the SDP context, the DP recursion is only ran once for each test day, so it is reasonable to test all grids in the table for this method.

This analysis was executed for two days: January 16th and July 27th. The results are shown in Figure 5-4: the peak shaving performance is shown in Figure 5-4a, and the recursion and control times in Figure 5-4b. In both figures, the x-axis scale is logarithmic, as the total number of evaluation points in Table 5-1 increases in orders of magnitude.

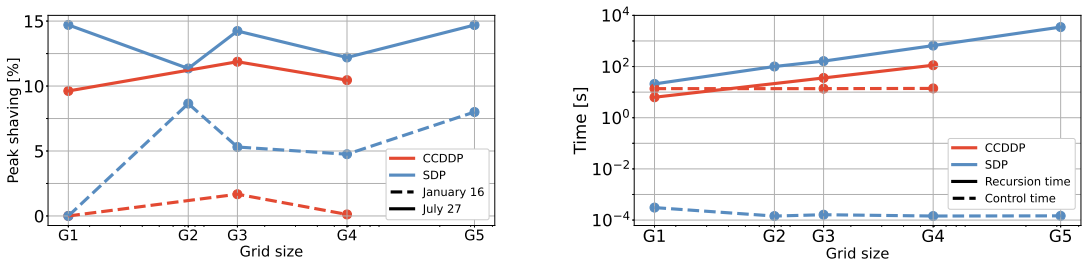

(a) **(b)**

Figure 5-4: Sensitivity and run-time analysis: (a) CCDDP method; (b) SDP method.

Figure 5-4a reaffirms that the SDP method performs better than the CCDDP method, in general. It also suggests that, for this particular data set, increasing the number of discretization points does not necessarily produce better peak shaving results. However, this might not hold for demand profiles with different characteristics, that require finer grids to capture their proper nature.

From Figure 5-4b we conclude that, for both methods, the recursion time increases linearly with the grid size (note that both axis are in logarithmic scale), although for the SDP method the recursion takes almost 10 times longer than the CCDDP recursion, irrespective of the grid size. We also note that the control time is mostly invariant through the several grids. Nevertheless, for the CCDDP method the control time is considerably larger than the control time of SDP ($\sim$13 seconds versus $\sim$1 millisecond), which is expected given that the CCDDP method calculates $K = 364$ coefficients in real-time.

This analysis suggest one major advantage of the CCDDP method versus the SDP method, with respect to run times. The proposed SDP method derives a model of the exogenous information for each target day based on the $K = 60$ previous profiles, and then computes an optimal policy in a one-day-ahead fashion, given this model. This could become intractable in terms of time for finer grids. On the other hand, provided that there exists a database of deterministic optimal policies which have been computed beforehand, the CCDDP method can still quickly be used to control the system in real-time —there are 15 minutes available between each decision epoch, and computing an optimal action takes around 13 seconds. Furthermore, updating the deterministic optimal policy database is fairly quick: for G4, calculating one new deterministic optimal policy takes $\sim$100 seconds (1.7 minutes). Assuming that the recursion time of the CCDDP method keeps its linear behaviour, for G5 it would take $\sim$ 400 seconds (6.7 minutes), which is still very optimistic. Therefore, even thought the SDP method gives better peak shaving performance, the CCDDP method may be more advantageous.

5-3 Summary and future work

In this work, two methods were proposed to perform peak shaving of daily demand profiles of an electricity consumer. Figure 5-5 shows a diagram summarizing the two methods.

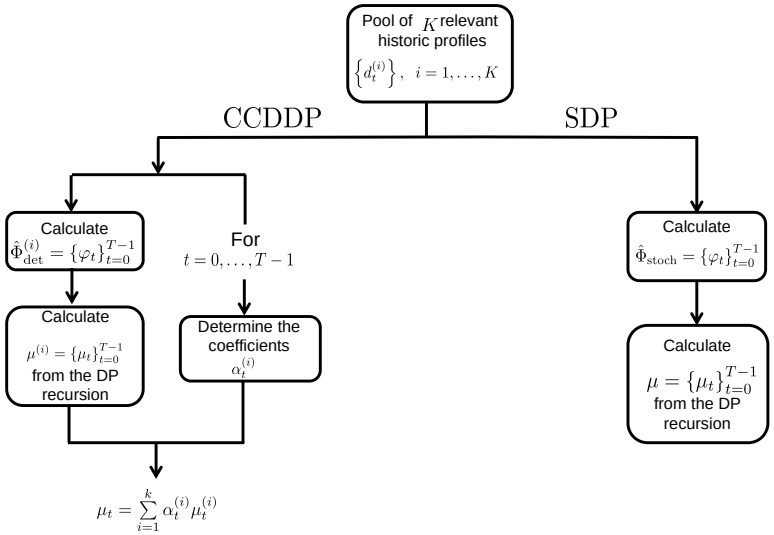

Figure 5-5: Diagram of the two proposed methods: CCDDP and SDP.

Both proposed methods show mostly successful peak shaving performances. Nevertheless, neither is immune to the occasional occurrence of peak increases. A peak increase may occur, for example, if the peak is too long and the battery capacity cannot keep up. In such scenario, it is possible that the control policy sends the battery a charging command mid-peak, leading to an increase in peak demand. Peak increases may also occur if the historic data available is a poor representative of the target profile. In order to prevent these events, we developed three simple modifications to be applied to either method, at control time, to increase their reliability. One of the proposed alterations, the $z^{\max}$-alteration, was particularly successful in avoiding peak increases in our numerical study with real data. In general, the SDP method produces better results than the CCDDP method. This is more evident when the methods are tested on real data than on artificially generated profiles. Depending on the computational power of available computers, however, the CCDDP method may prove to be advantageous, relative to the SDP.

In this work, time-of-use tariffs were not considered in the optimization, so there is a possibility that energy consumption is being shifted to times of the day when energy is more expensive. To guarantee that the electricity bill is reduced, time-of-use tariffs should be included into the optimal control problem via the stage cost function.

In order to extend battery lifespan, future works should consider studying appropriate constraints on the SoC, as has been done in literature [19, 20]. Abrupt variations between two consecutive commands should also be avoided so as to reduce battery stress. This could be done by extending the state of the system to include the previous action as an extra state variable and penalizing large differences between two consecutive inputs via the stage cost function.

Figure 4-5a tells us that, when applied to the CCDDP method, the ε-alteration pushes the median of peak shaving percentages upwards by around 2.5%. Future works could consider combining the ε- and $z^{\max}$- alterations in this order.

Figure A-1 in Appendix A shows the probabilistic model obtained for July 27th from the previous 60 days, for the time step corresponding to 9 o'clock in the morning. This figure suggests that, at 9AM, the tendency is that the consumer demand at 9:15 will be close to that of 9:00, since most probabilities are concentrated around $z = 0$. In order to attain more accurate models of the exogenous information, adaptive bounds $d^{\max}$, $z^{\min}$ and $z^{\max}$ could be considered, while keeping the same number of quantization points. Throughout this work, the lower bound on the demand was taken to be 0, but this approach could also take a positive lower bound $d^{\min}$. A simple way to do this would be to get these bounds from the pool of "relevant" profiles, instead of from the entire data set, as has been done in this work.

Further studies on this topic could analyse whether or not doing a forecast of the day ahead and selecting the relevant profiles based on this forecast would improve the results obtained in this work. Given a good forecast of the target day, the pool of relevant profiles could be composed of all profiles in the data set with an Euclidean distance to the forecast smaller than some threshold value, or the K profiles in the data set with the smallest Euclidean distances.

Appendix A

Stochastic model of the exogenous information

Algorithm 5 Stochastic model of z_{t+1}

Input:

pool of k historical demand profiles, $\left\{d_t^{(i)}\right\}_{t=0}^{T-1}, i = 1, \ldots, k$

Output:

stochastic model of the random variable, $\hat{\Phi}^{\text{stoch}}$

initialize $A_t^{(i)} = \{0\}^{N_d \times N_z}, i = 1, \ldots, k$
initialize $\varphi_t = \{0\}^{N_d \times N_z}$

for $t = 1, \ldots, T-1$ **do**

# GENERATE EACH INDIVIDUAL MATRIX
for $i = 1, \ldots, k$ **do**

$$row = \frac{\Pi_{\mathbb{D}_s}\left(d_t^{(i)}\right)}{{}^{d^{\max}}/_{N_d}}, \qquad col = \frac{\Pi_{\mathbb{Z}_s}\left(d_{t+1}^{(i)} - d_t^{(i)}\right)}{{}^{(z^{\max} - z^{\min})}/_{N_z}}$$

$$A_t^{(i)}(row, j) = 1e^{-4}, \qquad j = 1, \ldots, N_z$$

$$A_t^{(i)}(row, col) = A_t^{(i)}(row, col) + 1$$

end for

# COMBINE INDIVIDUAL MATRICES INTO A SINGLE MATRIX
for $row = 1, \ldots, N_d$ **do**

$$A_t(row, j) = \sum_{i=1}^{k} A_t^{(i)}(row, j), \qquad j = 1, \ldots, N_z$$

end for

FILL ROWS WITH ONLY ZEROS
Initialize $\varphi_t = A_t$
for $row = 1, \ldots, N_d$ **do**
Determine $d = \frac{row}{N_d - 1} d^{\max}$
if $\sum_{j=1}^{N_z} \varphi_t(row, j) = 0$ **then**

$$\alpha^r = \frac{1}{|row - r|} \qquad r \in \{1, \ldots, N_d\} \setminus row$$

$$\varphi_t(row, j) = \sum_{r \in \{1, \ldots, N_d\} \setminus row} \alpha^r \varphi_t(r, j), \qquad j = 1, \ldots, N_z$$

end if
end for

ALL PROBABILITIES MUST LEAD TO POSSIBLE EVENTS

# Find the column where the non-allowable probabilities should be accumulated
for $row = 1, \ldots, N_d$ **do**
  if $d + z^{\min} < 0$ **then**

    # The left-hand side of row must become zeros until demand constraints are satisfied
    $j = 0$
    while condition is true **do**
      $j+ = 1$
      $z = z^{\min} + \frac{j}{N_z - 1} z^{\max}$
      if $d + z >= 0$ **or** $j >= N_z - 1$ **then**
        col* = j
        condition is false
      end if
    end while
  else if $d + z^{\max} > d^{\max}$ **then**

    # The right-hand side of row becomes zeros if demand constraints are not satisfied
    Initialize $j = N_z$
    while condition is true **do**
      $j- = 1$
      $z = z^{\min} + \frac{j}{N_z - 1} z^{\max}$
      if $d + z >= 0$ **or** $j >= N_z - 1$ **then**
        $col* = j$
        condition is false
      end if
    end while
  end if

  # Accumulate non-allowable probabilities in col^*
  Initialize $temp = 0$
  for $col = 1, \ldots, N_z$ **do**
    $z = z^{\min} + \frac{col}{N_z - 1} z^{\max}$
    if $d + z < 0$ **or** $d + z > d^{\max}$ **then** # Out of bounds
      $temp = temp + \varphi_t(row, col)$
      $\varphi_t(row, col) = 0$
    end if
  end for
  # Normalize row
  $A_t(row, j) = \frac{A_t(row,j)}{\sum_{jj=1}^{N_z} A_t(row,jj)}, \qquad j = 1, \ldots, N_z$
  $\varphi_t(row, col^*) = \varphi_t(row, col^*) + temp$
end for
$\hat{\Phi}_{\text{stoch}} = \{\varphi_t\}_{t=0}^{T-1}$

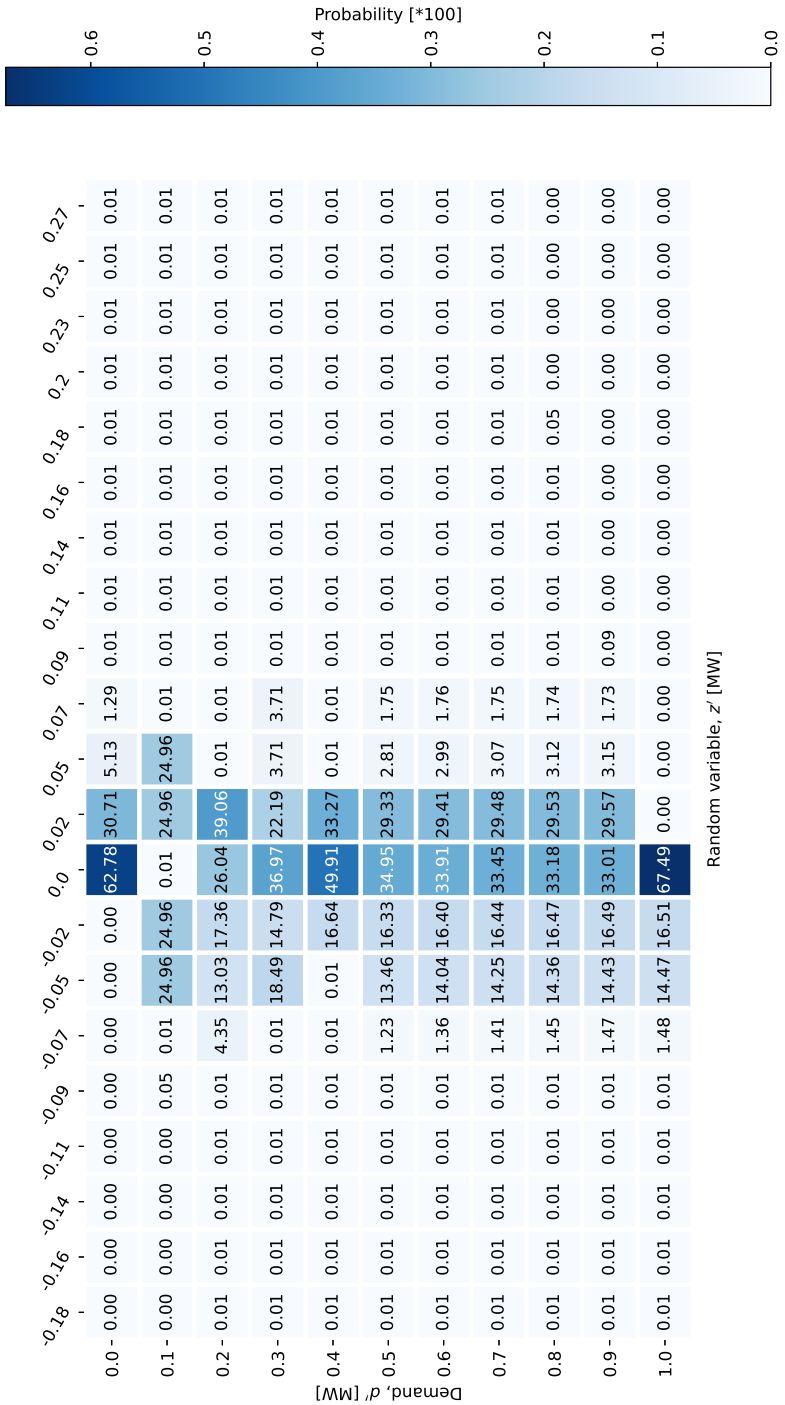

Figure A-1: Probabilistic model of the exogenous information obtained from the 60 demand profiles observed prior to July 27th, at 9 AM.

Appendix B

Data set

In Figure B-1, we plot the demand data by day of the year and by time of the day. It is possible to observe the variation of demand throughout the year —the days in the first and last months of the year are represented by much darker shades of blue —but also throughout the day —note one peak at around 9:00 and another at 18:00.

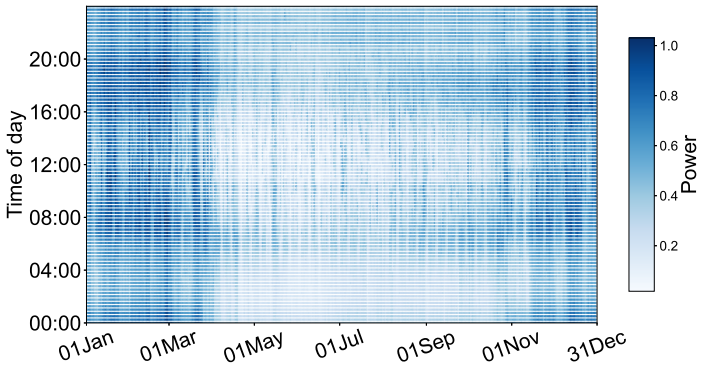

Figure B-1: Demand data by day of year and time of day

Appendix C

Deterministic results

It is interesting to see how the peak shaving methods perform when we assume full knowledge of the demand patterns' behaviour, i.e., when we consider the daily demand profiles in the data set to be deterministic paths, as the DP algorithm solves the optimal control problem for the exact profile. In other words, the DP results obtained with deterministic models of the exogenous information as defined in Eq. (3-2) give an idea of the best results we can expect, given a certain discretization grid. Note that the peak shaving percentages achieved with such models can not be realistically expected because the exact demand shape is not known in advance.

Figure C-1 shows the peak shaving results obtained for every day in the year 2018 from the DP algorithm using deterministic models of z_{t+1} for each day. The variables involved in the problem are quantized according to the number of points featured in Table 4-1. The figure shows the results in a histogram as well as in a box plot.

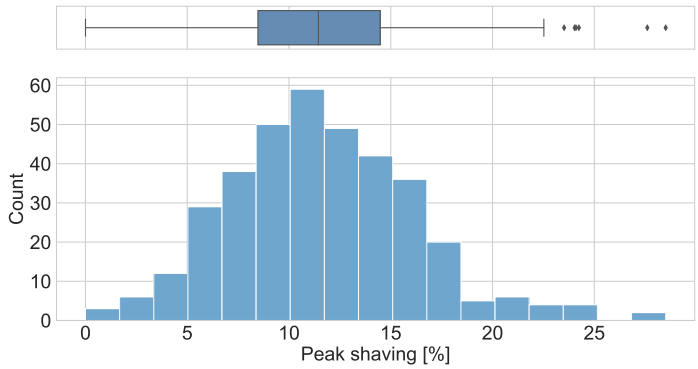

Figure C-1: Peak shaving results for all days of 2018 obtained from DP recursion with deterministic models of z.

The vertical line inside the box indicates the median of peak shaving values. The lowest 25% of data points are covered by the left whisker and the highest 25% are covered by the right

whisker. The box covers the middle 50% of the peak shaving values. The diamond shapes on the right-hand side of the box plot are outlier values. The median is located at 11.44%. The minimum value is 0, which means that there is at least one day where the peak is not shaved. It also means that, using deterministic models of the exogenous information, the DP method cannot possibly generate a peak increase. With deterministic solutions the DP recursion achieves peak shaving values up to around 22%, with some outlier cases going up to approximately 27%.

Appendix D

Effect of changing parameters W and K in the CCDDP method

.

Table D-1 shows the effect that changing the parameters W and K used in the CCDDP method has on the peak shaving performance. Tests were ran for two days: January 16th, in the winter, and July 27th, in the summer. The results shown in the table were obtained using 2-norm based coefficients $\alpha_t^{(i)}$. Note that the pool is composed of the K most recent daily profiles.

We can see that, for any fixed value of K, the peak shaving results do not suffer a lot of variation, regardless of the length W of the time windows w_t and $w_t^{(i)}$. However, changing the size of the pool of relevant data improves the performance of the method for the two days tested.

Table D-1: Effect of changing parameters W and K in the CCDDP method.

	January 16th	July 27th
Original: $W = 16, K = 364$	0.578%	11.603%
$W = 8, K = 364$	0.409%	11.783%
$W = 32, K = 364$	0.515%	11.208%
$W = 32, K = 60$	1.767%	14.176%
$W = 16, K = 60$	1.789%	14.387%
$W = 8, K = 60$	1.812%	**14.558 %**
$W = 32, K = 10$	1.496%	13.616%
$W = 16, K = 10$	1.589%	14.255%
$W = 8, K = 10$	**1.826 %**	14.242%

Appendix E

Distributions of p-norm distances and p-norm based coefficients

In Section 4-3, we have speculated that the p-norm based coefficients produce similar peak shaving results, regardless of the value of p due to the inversion and normalization processes. This claim is supported by the figures below.

To generate the figures, the p-norm distances, $\delta_{p,t}^{(i)}$, and the p-norm based coefficients, $\alpha_t^{(i)}$, were obtained for each time step $t \in \{0,\ T\}$ for two days January 16th and July 27th. Hence, there is a total of $T \cdot K \cdot 2 = 69,888$ coefficients for each value of p.

Figure E-1 shows the histograms of the two variables obtained for each variable, with the p-norm distance in Figure E-1a and the p-norm based coefficients in Figure E-1b. Note that the distributions of distance are significantly different for the different values of p, while the distributions of the coefficients are very similar.

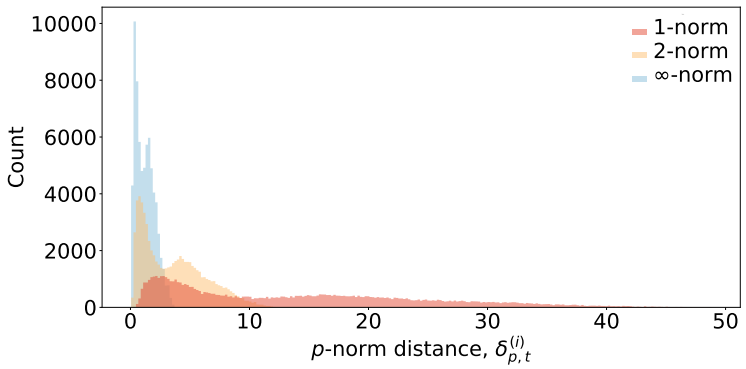

(a) **(b)**

Figure E-1: Distributions of distance and coefficients: (a) p-norm distances; (b) p-norm based coefficients.

Appendix F

Effect of a different similarity measure in CCDDP method

Figure F-1 shows the effect of peak duration and similarity between the target profile and the pool of historical data. In the figure below, similarity is measured in a different way than in Section 5-1. At each time, K Euclidean distances between $w_t^{(0)}$ and $w_t^{(i)}$ $, i \in \{1, 2, \ldots, K\}$ are calculated. Then, a weighted average of these distances is calculated, where the weights are the coefficients $\alpha_t^{(i)}$,

$$\overline{\delta}_t = \sum_{i=1}^{K} \alpha_t^{(i)} \delta_t^{(i)} \tag{F-1}$$

where $\delta_t^{(i)}$ is the Euclidean distance between $w_t^{(0)}$ and $w_t^{(i)}$. An average Euclidean distance $\overline{\delta}_t$ is calculated for all $t \in \{0, 1, \ldots, T\}$. Then, all T average Euclidean distances are averaged, this time with uniform weights,

$$\overline{\delta} = \frac{1}{T} \sum_{t=0}^{T} \overline{\delta}_t. \tag{F-2}$$

Similarity is given as the inverse of the average Euclidean distance between that day and days in the pool.

Given this similarity measure, which captures exactly how the CCDDP method approximated the target profile from historic data, the pattern observed before where peak shaving performance increases for larger similarities becomes evident.

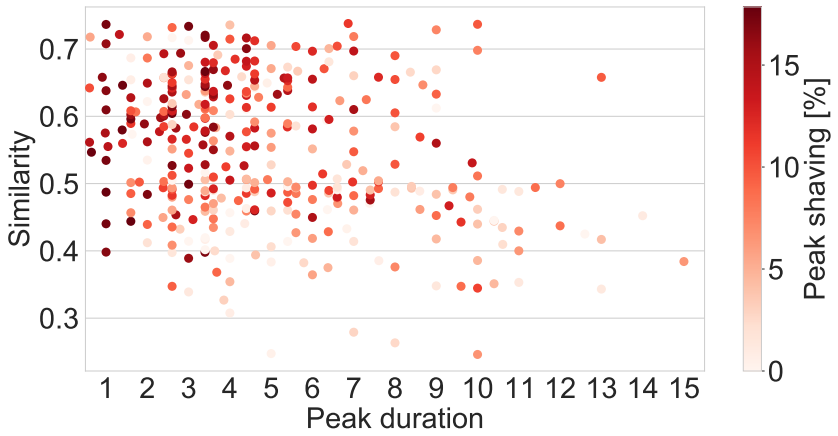

Figure F-1: Effect of peak duration and representativity in peak shaving performance of the CCDDP method. Similarity is measured weighted by the coefficients.

Bibliography

[1] A. Gajduk, M. Todorovski, and L. Kocarev, "Stability of power grids: An overview," *The European Physical Journal Special Topics*, vol. 223, pp. 2387–2409, 06 2014.

[2] K. A. Joshi and N. M. Pindoriya, "Day-ahead dispatch of battery energy storage system for peak load shaving and load leveling in low voltage unbalance distribution networks," in *2015 IEEE Power Energy Society General Meeting*, pp. 1–5, 2015.

[3] P. Palensky and D. Dietrich, "Demand side management: Demand response, intelligent energy systems, and smart loads," *IEEE Transactions on Industrial Informatics*, vol. 7, pp. 381–388, Aug. 2011.

[4] C. C. Thompson, P. E. Konstantinos Oikonomou, A. H. Etemadi, and V. J. Sorger, "Optimization of data center battery storage investments for microgrid cost savings, emissions reduction, and reliability enhancement," *IEEE Transactions on Industry Applications*, vol. 52, no. 3, pp. 2053–2060, 2016.

[5] Eurelectric, "The role of electricity," tech. rep., The Union of the Electricity Industry, 2007.

[6] S. Mishra and P. Palanisamy, "Efficient power flow management and peak shaving in a microgrid-pv system," *Proceedings of the international conference on renewable energy and sustainable devlopment*, 2013.

[7] M. Zheng, C. J. Meinrenken, and K. S. Lackner, "Smart households: Dispatch strategies and economic analysis of distributed energy storage for residential peak shaving," *Applied Energy*, vol. 147, pp. 246 – 257, 2015.

[8] K. H. Chua, Y. S. Lim, and S. Morris, "Cost-benefit assessment of energy storage for utility and customers: A case study in malaysia," *Energy Conversion and Management*, vol. 106, pp. 1071 – 1081, 2015.

[9] U. D. of Energy, "The smar grid: an introduction," tech. rep., 2008.

[10] A. Oudalov, D. Chartouni, C. Ohler, and G. Linhofer, "Value analysis of battery energy storage applications in power systems," *2006 IEEE PES Power Systems Conference and Exposition*, pp. 2206–2211, 2006.

[11] A. Barbato and A. Capone, "Optimization models and methods for demand-side management of residential users: A survey," *Energies*, vol. 7, pp. 5787–5824, 09 2014.

[12] R. Martins, H. Hesse, J. Jungbauer, T. Vorbuchner, and P. Musilek, "Optimal component sizing for peak shaving in battery energy storage system for industrial applications," *Energies*, vol. 11, p. 2048, 08 2018.

[13] M. Uddin, M. F. Romlie, M. F. Abdullah, S. Abd Halim, A. H. Abu Bakar, and T. Chia Kwang, "A review on peak load shaving strategies," *Renewable and Sustainable Energy Reviews*, vol. 82, pp. 3323 – 3332, 2018.

[14] J. Eyer and G. Corey, "Energy storage for the electricity grid: Benefits and market potential assessment guide," pp. 1–232, 01 2011.

[15] S. Zachary, S. Tindemans, M. Evans, J. Cruise, and D. Angeli, "Scheduling of energy storage," 2020.

[16] A. Oudalov, R. Cherkaoui, and A. Béguin, "Sizing and optimal operation of battery energy storage system for peak shaving application," pp. 621 – 625, 08 2007.

[17] R. Sioshansi, S. H. Madaeni, and P. Denholm, "A dynamic programming approach to estimate the capacity value of energy storage," *IEEE Transactions on Power Systems*, vol. 29, no. 1, pp. 395–403, 2014.

[18] K. H. Chua, Y.-S. Lim, and S. Morris, "Battery energy storage system for peak shaving and voltage unbalance mitigation," *International Journal of Smart Grid and Clean Energy*, vol. 2, pp. 357–363, 01 2013.

[19] A. Lucas and S. Chondrogiannis, "Smart grid energy storage controller for frequency regulation and peak shaving, using a vanadium redox flow battery," *International Journal of Electrical Power Energy Systems*, vol. 80, pp. 26 – 36, 2016.

[20] J. Leadbetter and L. Swan, "Battery storage system for residential electricity peak demand shaving," *Energy and Buildings*, vol. 55, pp. 685 – 692, 2012. Cool Roofs, Cool Pavements, Cool Cities, and Cool World.

[21] G. Karmiris and T. Tengnér, "Peak shaving control method for energy storage," 2013.

[22] E. Reihani, M. Motalleb, R. Ghorbani, and L. Saad Saoud, "Load peak shaving and power smoothing of a distribution grid with high renewable energy penetration," *Renewable Energy*, vol. 86, pp. 1372 – 1379, 2016.

[23] D. P. Bertsekas, *Dynamic Programming and Optimal Control.* Athena Scientific, 3rd ed., 2005.

[24] W. B. Powell, *Approximate dynamic programming: solving the curses of dimensionality.* Wiley-Interscience, 1st ed., 2007. ISBN:978-0470171554.

[25] R. E. Bellman, *Dynamic Programming*. Dover Publications, Inc., 2003.

[26] R. Bellman, "Dynamic programming and stochastic control processes," *Information and Control*, vol. 1, no. 3, pp. 228 – 239, 1958.

[27] "Implementation of dynamic programming for optimal control problems with continuous states," *IEEE Transactions on Control Systems Technology*, vol. 23, pp. 1172–1179, May 2015.

[28] S. P. Bradley, A. C. Hax, and T. L. Magnanti, *Applied Mathematical Programming*. Addison-Wesley Publishing Company, 1977.

[29] G. A. Hanasusanto and D. Kuhn, "Robust data-driven dynamic programming," in *NIPS*, pp. 827–835, 2013.

[30] J. W. Taylor, "Triple seasonal methods for short-term electricity demand forecasting," *European Journal of Operational Research*, vol. 204, no. 1, pp. 139 – 152, 2010.

[31] A. I. Khuri, "Applications of dirac's delta function in statistics," *International Journal of Mathematical Education in Science and Technology*, vol. 35, no. 2, pp. 185–195, 2004.

[32] M. Verhaegen and V. Verdult, *Filtering and System Identification: A Least Squares Approach*. Cambridge University Press, 2007.

Nomenclature

List of Symbols

Abbreviations

CCDDP	Convex combination from dynamic programming.
DP	Dynamic program, or dynamic programming.
SDP	Stochastic dynamic programming.

Latin Symbols

ℓ	Load on the grid.
$\mathbb{E}(\cdot)$	Expected value.
$\mathbb{P}(\cdot)$	Probability.
c	State-of-charge.
d	Power demand.
f	State dynamics.
G	Terminal cost.
g	Stage cost.
J	Value function.
K	Number of profiles in the pool of relevant data.
p	Peak load.
ps	Peak shaving percentage.
u	Action.
W	Length of the moving window.
w_t	Sub-profile of length W.
x	State vector.
z	Exogenous information.

Greek Symbols

$\alpha_t^{(i)}$	Coefficient of a convex combination.
μ	Optimal policy.
$\overline{\alpha}$	Charging rate.
Φ	Model of the exogenous information.
$\underline{\alpha}$	Discharging rate.

Subscripts

T	Final time instant.
t	Current time instant.
$t+1$	Next time instant.
det	Deterministic.
stoch	Stochastic.

Superscripts

max	Maximum value of variable.
min	Minimum value of variable.
*	Optimal.